Preparing prehydrolyzed kraft dissolving pulp via phosphotungstic acid prehydrolysis from grape branches

LI TAO, MA YING HUA, AND ZHANG JUN KE

ABSTRACT: Dissolving pulp was successfully prepared via phosphotungstic acid (PTA) prehydrolysis kraft (PHK) cooking followed by an elemental chlorine-free (ECF) bleaching process from grape branches. The effects of prehydrolysis temperature, reaction time, and PTA concentration that potentially affect the quality of dissolving pulp product on chemical components of pulp were studied via an orthogonal experiment. The structure of lignin was activated during the PTA prehydrolysis phase, and lignin was easily removed during the following cooking process. Thus, relatively mild conditions (140°C, 100 min) can be used in the cooking process. During the prehydrolysis phase, temperature exhibited the most significant influence on the cellulose purity of the obtained pulp fiber, followed by reaction time and PTA concentration. The optimized prehydrolysis conditions were as follows: prehydrolysis temperature, 145°C; reaction time, 75 min; and PTA concentration, 1 wt%. Whether the excessively high prehydrolysis temperature or prolonging the reaction time did not favor the retention of long chain cellulose, the delignification selectivity for the cooking process could not be further improved by excessive PTA loading. Under these prehydrolysis conditions, 94.1% and 29.0% for α-cellulose content and total yield could be achieved after the given cooking and bleaching conditions, respectively. Moreover, the chemical structure and crystal form of cellulose were scarcely changed after PTA prehydrolysis, which could be confirmed by results from Fourier transform infrared (FTIR) spectroscopy and X-ray diffraction (XRD). PTA prehydrolysis could be considered as an alternative method for preparing PHK dissolving pulp under relatively mild cooking conditions.

Application: Phosphotungstic acid prehydrolysis presents an alternative approach for preparing a PHK dissolving pulp product, as well as solving the acid recovery problem during the PHK process.

Dissolving pulp is a kind of purified chemical pulp with high α-cellulose content. It can be used as the feedstock for many high value-added cellulose products, such as viscose fiber, cellophane, cellulose ester, and/or ether. Dissolving pulp is mainly produced via a prehydrolysis kraft (PHK) process or acid sulfite (AS) process. The amount of dissolving pulp produced by these two methods accounts for 85% to 88% of the total dissolving pulp production all over the world, whereas the pulp obtained via the AS process exhibits a wider distribution of polymerization degree than that from the PHK process and a relatively higher requirement for raw materials. Until now, the PHK process, which has a wide range of feedstock from which to select, is usually adopted for newly-built production lines of dissolving pulp [1,2]. During the PHK process, part of the hemicelluloses and lignin can be degraded and removed from raw materials, and the reactivity of lignin can also be improved by the prehydrolysis process, which favors the removal of lignin during the subsequent cooking process. Many studies on prehydrolysis of wood chips or other raw materials have been reported, for example, dilute acid prehydrolysis [3] and hot water extraction [4]. Dilute acid prehydrolysis (0.5%–10%) was once widely considered due to its good economy and high efficiency, though subsequent equipment corrosion and acid recovery hindered its further development [5].

As a new and emerging type of solid heteropoly acid catalyst, phosphotungstic acid (PTA) exhibits some unique physicochemical properties, including strong Brønsted acidity, proton mobility, low corrosion to equipment, high stability, and reusability [6]. Due to these special characteristics, PTA was used to depolymerize cellulose to platform chemicals [7,8] or to realize viscosity control and accessibility/reactivity improvement for dissolving pulp [9], and even to prepare nanocellulose-based materials [10]. The depolymerization effect of PTA on hemicelluloses was also reported. The enzymolysis efficiency of cellulase for agricultural biomass could be remarkably improved via PTA pretreatment [11,12]. Moreover, solid heteropoly acids are insoluble in nonpolar hydrocarbons, making it possible to recover them from the reaction mixture without the need for neutralization and simply by extraction or precipitation [13]. As reported, lignin can be depolymerized into phenolic monomers under the catalytic effect of solid heteropoly acids [14,15]. Moreover, the catalytic effect of solid heteropoly acids

combined with neutral deep eutectic solvent [16] or MCM-41 zeolite [17] on lignin macromolecules was also reported. Since the structure of a lignin macromolecule can be activated and/or depolymerized by incorporating solid heteropoly acids under varied conditions, it is reasonable to infer that solid heteropoly acid catalysts can be used to replace dilute acid prehydrolysis for a dissolving pulp preparation and can be expected to solve the acid recovery problem during the PHK process.

At present, many studies have been made for expanding the material source of dissolving pulp. Global demand for dissolving pulp has been increasing at a remarkable pace over the last few years [18]. China is the biggest consumer of dissolving pulp in the world. Nonetheless, more than 50% of the consumption of dissolving pulp relies on imports [2]. As a kind of widely planted agricultural product, the cultivated area of grapes has been increasing year by year in China. As reported, the cultivated area exceeded one million hectares in 2020. As a result, increased grape pruning has increased the land accumulation of pruning residual, as well as pollution from burning it. With the goal of expanding the raw material source for preparing dissolving pulp and solving the pollution caused by grape pruning residual, the PHK process using grape branches via PTA prehydrolysis was investigated. The effects of prehydrolysis temperature, reaction time, and PTA concentration that potentially affect the quality of the dissolving pulp product were studied via an orthogonal experiment. Moreover, the morphological and structural characteristics of specimens after PTA prehydrolysis and cooking were also analyzed.

EXPERIMENTAL

Materials

Grape branches, with average length of about 20–30 mm and average diameter of 7–12 mm, were provided by the Agricultural Bureau of Xunyi District, Xi'an, China. The chemical components of the grape branches (w/w) were as follows: holocellulose, 65.45%; Klason lignin, 26.83%; acid-soluble lignin, 0.55%; pentosane, 14.13%; and benzene-alcohol extractive, 5.48%.

Phosphotungstic acid ($H_3O_{40}PW_{12}$) (PTA, AR); ammonium ferrous sulfate [$(NH_4)Fe(SO_4)_2{\cdot}6H_2O$, AR]; potassium dichromate ($K_2Cr_2O_7$, AR); sulfuric acid (H_2SO_4, purity≧98.0%); sodium hydroxide (NaOH, AR); hydrogen peroxide (H_2O_2, 36.5%); sodium metasilicate (Na_2SiO_3, AR); magnesium sulfate ($MgSO_4$, AR); acetic acid (CH_3COOH, AR); sodium chlorite ($NaClO_2$, AR); and potassium bromide (KBr, SP) were purchased from Tianli Chemical Co. Ltd. (Tianjin, China) and were used as received without further purification. Bis(ethylenediamine) copper(II) hydroxide solution (1 M in H_2O) was purchased from Sigma-Aldrich Co. Ltd. (Shanghai, China). The chlorine dioxide (ClO_2) solution was generated in the laboratory prior to performing the bleaching procedure.

Level	Factors		
	Prehydrolysis Temperature, °C	Reaction Time, min	PTA Concentration, %
1	110	25	0
2	125	50	1
3	140	75	2
4	155	100	3

I. Orthogonal experimental design parameters of prehydrolysis (PTA = phosphotungstic acid).

Methods

PTA prehydrolysis

PTA was prepared into aqueous solution with a certain concentration. Subsequently, around 150 g of grape branches (dry weight) and the required amount of PTA aqueous solution were added into a stainless steel reactor of 1000 mL volume, sealed, and put into a digester kier (ZQS1, machinery factory of Shaanxi University of Science and Technology, China). The wood-to-liquid ratio was 1:4. The system was heated to a pre-seated maximum temperature within 40 min, and then kept at the maximum temperature for a required duration. After prehydrolysis, specimens were washed until neutral with deionized water and air dried.

The main factors, including prehydrolysis temperature, reaction time, and PTA concentration, were investigated via an orthogonal experiment. The factors and levels of the orthogonal experiment are shown in **Table I**, and the treatment conditions for specimens are given in **Table II**. In addition, the untreated grape branches were named OS for further analysis.

Kraft cooking

All the selected specimens after PTA prehydrolysis were subjected to the kraft pulping process. The active alkali loading based on specimen was 16 wt%, and sulfidity was 18 wt%. The wood-to-liquid ratio was 1:4. The temperature in the reactor was raised from 25°C to 140°C within 40 min, and it was kept constant for 100 min. Kraft cooking was conducted in an oil-bath reactor (ZQS1, machinery factory of Shaanxi University of Science and Technology, China) that contained four rotating autoclaves of 1000 mL.

Bleaching sequences and conditions

An O-D_0–E_p–D_1 ECF bleaching was used to treat PHK pulp after cooking. Kraft pulp (10 g, as o.d. weight) was oxygen bleached at the pulp consistency of 30 wt%. After washing, the pulp was treated with ClO_2 in a polyethylene bag at the pulp consistency of 10 wt%, washed again, and treated in a polyethylene bag with NaOH and H_2O_2. Finally, the pulp was washed and treated with ClO_2 again.

Specimen	Prehydrolysis Temperature, °C	Reaction Time, min	PTA Concentration, %
1	110	25	0
2	110	50	1
3	110	75	2
4	110	100	3
5	125	25	1
6	125	50	0
7	125	75	3
8	125	100	2
9	140	25	2
10	140	50	3
11	140	75	0
12	140	100	1
13	155	25	3
14	155	50	2
15	155	75	1
16	155	100	0

II. Orthogonal experimental conditions of prehydrolysis (PTA = phosphotungstic acid).

The bleaching conditions were as follows:

- O phase: pulp consistency, 30 wt%; initial oxygen pressure, 0.5 MPa; NaOH loading, 5 wt%; $MgSO_4$ loading, 0.5 wt%; temperature, 95°C; reaction time, 60 min.
- D_0 phase: pulp consistency, 10 wt%; ClO_2 loading, 1.5 wt%; temperature, 75°C; reaction time, 90 min.
- E_p phase: pulp consistency, 10 wt%; NaOH loading, 1.0 wt%; H_2O_2 loading, 1.5 wt%; Na_2SiO_3 loading, 2.0 wt%; initial oxygen pressure, 0.5 MPa; temperature, 90°C; reaction time, 60 min.
- D_1 phase: pulp consistency, 10 wt%; ClO_2 loading, 0.5 wt%; temperature, 70°C; reaction time, 60 min.

Characterizations

The holocellulose and lignin contents of specimens were measured according to TAPPI Standard Test Method T 222 om-15 "Acid-insoluble lignin in wood and pulp." The α-cellulose content and alkali solubility (S_{10} and S_{18}) of delignified specimens were measured according to TAPPI T 203 cm-09 "Alpha-, beta- and gamma-cellulose in pulp" and TAPPI T 235 cm-09 "Alkali solubility of pulp at 25°C," respectively. The obtained results were defined as α-cellulose content and alkali solubility based on holocellulose, respectively. The average degree of polymerization (DP) of specimens was measured using the viscosity method according to TAPPI T 230 om-19 "Viscosity of pulp (capillary viscometer method)."

The α-cellulose content and alkali solubility (S_{10} and S_{18}) based on the specimen were calculated according to the following formula:

$$A = B * C$$

where A is the α-cellulose content/alkaline solubility (S_{18} or S_{10}-S_{18}) based on the specimen; B is the corresponding α-cellulose content/alkaline solubility based on holocellulose; and C is the holocellulose content based on this specimen.

The dried specimens were mixed with KBr and pressed into tablets. Then, analysis was performed using Fourier transform infrared (FTIR) spectroscopy (VERTEX-70; Bruker, Germany) in the range of 4000-400 cm^{-1} with a resolution of 4 cm^{-1}.

The X-ray diffraction (XRD) patterns were collected on a Bruker D8-Advance instrument (Karlsruhe, Germany) equipped with a Cu Kα radiation (k=1.54 A°) as an X-ray resource operating (40 kV, 30 mA) by a scan rate of 0.1° per second in a 2θ range of 10° to 60°.

The morphology of raw material and specimens was observed using a HITACHI S-8100 SEM (Hitachi; Tokyo, Japan) apparatus at 5.0 kV accelerating voltage. Before SEM measurement, the dried specimens were dispersed on double-sided conductive tape and sprayed with gold in a vacuum.

RESULTS AND DISCUSSION

Influences of process variables on chemical components

The influences of prehydrolysis process variables, including prehydrolysis temperature, reaction time, and PTA concentration, on the chemical components of specimens after prehydrolysis and cooking were investigated via an orthogonal experiment with four levels. The corresponding results are shown in **Table III** and **Table IV**, respectively. Moreover, the influences of process variables on the carbohydrate components after prehydrolysis and cooking calculated by range analysis are shown in **Figs. 1–3**. According to the range analysis, the influence order of process variables on the cellulose purity of obtained pulp fiber was as follow: prehydrolysis temperature > reaction time > PTA concentration.

Influences of prehydrolysis temperature

Figure 1 shows the influences of prehydrolysis temperature on carbohydrate contents of specimens after prehydrolysis and cooking. As indicated by Table III and Fig. 1a, both the yield and holocellulose content of specimens exhibited significant decrease with increasing temperature during the prehydrolysis phase, especially at 155°C, indicating the dra-

Specimens	Holocellulose Content, %	α-Cellulose Content, %		$S_{10'}$ %		$S_{18'}$ %		S_{10}-$S_{18'}$ %		Lignin Content, %		α-Cellulose Yield, %	Yield, %
		For Specimens	For Holo-cellulose	For Specimens	For Holo-cellulose	For Specimens	For Holo-cellulose	For Specimens	For Holo-cellulose	Acid Insoluble	Acid Soluble		
OS	65.45±2.53	51.93±0.51	79.34±0.78	14.88±0.58	22.73±0.88	13.55±0.23	20.70±0.35	1.33±0.81	2.33±1.23	26.83±0.42	0.55±0.08	-	-
1	71.29±1.97	52.18±0.99	73.20±1.40	14.27±0.45	20.02±0.63	12.20± 1.07	17.12±1.50	2.07±1.52	2.90±2.13	27.51±0.63	0.52±0.03	94.21±3.85	95.08±1.88
2	71.39±0.93	54.24±0.22	75.98±0.31	10.97±0.83	15.37±1.17	9.64±0.30	13.51±0.42	1.33±1.13	1.86±1.59	27.40±0.60	0.43±0.09	95.42±3.74	94.59±1.77
3	66.58±0.70	48.92±0.32	73.47±0.49	10.93±0.08	16.42±0.12	8.10±0.11	12.17±0.16	2.83±0.19	4.25±0.28	29.12±1.28	0.40±0.05	86.28±1.10	91.59±0.17
4	61.78±0.78	46.14±0.91	74.68±1.51	9.87±0.20	15.98±0.50	6.92±0.27	11.20±0.44	2.95±0.47	4.78±0.94	29.02±0.19	0.39±0.07	81.60±1.07	91.84±0.29
5	66.59±1.70	53.56±0.80	80.43±1.23	11.07±1.04	16.63±1.59	8.34±0.70	12.53±1.08	2.73±1.74	4.10±2.67	27.25±0.94	0.39±0.02	95.08±3.22	92.48±1.52
6	64.23±1.74	51.40±0.79	80.02±1.27	10.74±0.70	16.72±1.12	8.54±0.13	13.29±0.21	2.20±0.83	3.43±1.33	28.99±1.00	0.40±0.04	91.50±2.01	92.45±0.27
7	64.43±0.50	50.92±1.00	79.03±1.60	10.47±0.49	16.25±0.78	7.63±0.25	11.85±0.40	2.83±0.74	4.40±1.18	29.84±1.31	0.37±0.05	87.87±1.97	89.62±1.47
8	62.15±1.01	49.67±0.04	79.91±0.06	12.98±0.32	20.89±0.53	7.35±0.92	11.83±1.54	5.63±1.24	9.06±2.07	29.67±0.93	0.36±0.05	85.27±2.91	89.16±1.90
9	66.39±1.75	52.46±0.45	80.00±0.70	11.53±0.66	17.58±1.04	7.45±1.14	11.36±1.79	4.08±1.70	6.22±2.83	29.75±0.54	0.35±0.02	88.70±3.76	87.80±2.01
10	66.09±1.73	52.53±1.15	80.50±1.83	11.22±0.37	17.20±0.59	7.20±0.33	11.03±0.52	4.03±0.70	6.17±1.11	31.19±1.24	0.32±0.01	84.48±1.84	83.52±0.09
11	64.09±0.91	51.61±0.75	81.56±1.24	11.95±0.95	18.88±1.55	7.44±0.10	11.75±0.16	4.51±1.05	7.13±1.71	27.52±1.01	0.37±0.03	93.16±1.26	93.74±0.35
12	63.45±1.48	50.31±0.77	80.31±1.29	10.80±0.77	17.24±1.28	6.79±1.19	10.84±1.99	4.01±1.96	6.40±3.27	29.40±0.34	0.36±0.07	86.16±2.44	88.93±0.96
13	64.61±0.65	46.80±0.86	72.43±1.42	12.51±0.72	19.36±1.19	7.07±0.29	10.94±0.48	5.44±1.01	8.42±1.67	29.79±1.29	0.23±0.06	78.645±1.92	87.27±1.27
14	64.04±1.07	48.74±0.40	76.11±0.67	8.32±0.45	13.00±0.75	6.56±0.72	10.24±1.20	1.77±1.17	2.76±1.95	30.22±0.18	0.25±0.04	80.85±1.71	86.15±0.64
15	64.46±1.05	51.47±1.11	79.86±1.85	11.63±0.99	18.05±1.65	5.92±0.27	9.18±0.46	5.72±1.26	8.87±2.11	32.24±0.88	0.28±0.02	79.37±2.17	80.07±1.12
16	63.55±0.50	51.47±1.07	81.00±1.83	9.16±0.99	14.41±1.69	3.95±0.50	6.22±0.86	5.20±1.49	8.19±2.55	32.84±0.35	0.33±0.05	77.32±2.32	78.01±1.82

III. Chemical components of specimens after prehydrolysis (OS = untreated grape branch).

Specimens	Holocellulose Content, %	α-Cellulose Content, %		$S_{10'}$ %		$S_{18'}$ %		S_{10}-$S_{18'}$ %		Lignin Content, %		α-Cellulose Yield, %	Yield, %	Dissociated to Fiber, Yes/No
		For Specimens	For Holo-cellulose	For Specimens	For Holo-cellulose	For Specimens	For Holo-cellulose	For Specimens	For Holo-cellulose	Acid Insoluble	Acid Soluble			
1	57.45±1.22	54.27±0.11	94.46±0.19	6.28±0.03	10.93±0.06	2.96±0.09	5.16±0.16	3.31±0.12	5.77±0.22	35.92±1.16	0.18±0.03	48.20±2.54	43.85±1.32	N
2	63.55±1.22	59.55±0.06	93.71±0.10	6.22±0.01	9.78±0.01	3.53±0.03	5.55±0.05	2.69±0.04	4.23±0.06	26.55±2.03	0.18±0.01	52.34±3.28	43.17±2.06	N
3	75.34±1.10	70.75±0.78	93.91±1.04	6.87±0.05	9.12±0.06	4.17±0.03	5.53±0.04	2.70±0.08	3.59±0.10	18.03±0.96	0.17±0.04	62.51±1.68	42.02±0.58	N
4	68.86±0.66	64.90±0.18	94.25±0.26	5.77±0.08	8.38±0.12	3.53±0.03	5.13±0.05	2.24±0.12	3.25±0.17	27.08±1.11	0.17±0.02	57.93±1.90	42.57±1.24	N
5	82.66±0.87	78.17±0.04	94.57±0.05	6.90±0.01	8.35±0.01	4.10±0.13	4.96±0.16	2.80±0.14	3.390.17	13.17±1.02	0.15±0.02	61.75±2.07	37.94±1.20	Y
6	68.52±0.07	65.35±0.69	95.38±1.00	6.30±0.11	9.19±0.16	3.89±0.08	5.68±0.11	2.41±0.29	3.51±0.28	23.08±0.91	0.15±0.03	52.00±0.49	38.20±0.42	N
7	75.11±1.43	70.99±0.14	94.52±0.18	5.92±0.10	7.88±0.13	3.11±0.11	4.14±0.15	2.81±0.21	3.74±0.28	16.53±0.85	0.14±0.05	54.25±1.61	35.56±0.18	Y
8	79.78±1.90	74.94±0.45	93.93±0.56	6.85±0.10	8.59±0.12	1.99±0.14	2.50±0.17	4.86±0.24	6.09±0.29	14.78±1.11	0.13±0.01	53.52±2.06	33.07±0.16	Y
9	87.30±0.43	82.43±1.27	94.42±1.45	6.40±0.04	7.33±0.05	3.58±0.10	4.10±0.12	2.82±0.14	3.23±0.17	10.52±0.83	0.12±0.02	55.86±2.42	30.90±1.99	Y
10	91.44±1.87	85.91±0.38	93.95±0.42	6.75±0.16	7.38±0.17	2.52±0.12	2.76±0.13	4.22±0.28	4.62±0.30	7.63±0.88	0.11±0.02	53.78±2.61	27.15±0.74	Y
11	83.97±1.91	79.78±0.18	95.01±0.21	6.94±0.07	8.26±0.08	2.94±0.16	3.50±0.19	4.00±0.23	4.76±0.27	13.85±1.20	0.11±0.01	50.68±3.58	30.92±1.67	Y
12	90.08±1.61	85.97±0.02	95.43±0.02	6.13±0.15	6.81±0.17	2.82±0.02	3.13±0.02	3.32±0.17	3.68±0.19	6.08±1.02	0.12±0.01	53.73±3.65	28.87±2.04	Y
13	92.75±0.04	86.99±1.16	93.79±1.25	6.85±0.19	7.39±0.20	1.96±0.05	2.11±0.05	4.90±0.24	5.28±0.25	3.59±0.71	0.11±0.05	45.18±0.83	23.54±0.79	Y
14	96.79±1.18	91.71±1.05	94.75±1.08	5.76±0.06	5.95±0.06	1.98±0.12	2.05±0.12	3.77±0.28	3.90±0.18	0.93±0.08	0.1±0.03	50.93±1.49	24.85±0.31	Y
15	96.44±0.94	91.44±1.60	94.82±1.66	5.89±0.14	6.11±0.14	1.46±0.16	1.51±0.17	4.44±0.30	4.60±0.31	1.17±0.93	0.11±0.03	51.10±3.15	23.24±2.21	Y
16	88.59±1.39	84.38±1.13	95.25±1.28	6.99±0.13	7.89±0.15	3.04±0.17	3.43±0.19	3.95±0.30	4.46±0.34	7.09±0.28	0.12±0.05	51.10±1.63	24.53±0.24	Y
16	63.55±0.50	51.47±1.07	81.00±1.83	9.16±0.99	14.41±1.69	3.95±0.50	6.22±0.86	5.20±1.49	8.19±2.55	32.84±0.35	0.33±0.05	77.32±2.32	78.01±1.82	

IV. Chemical components of specimens after cooking.

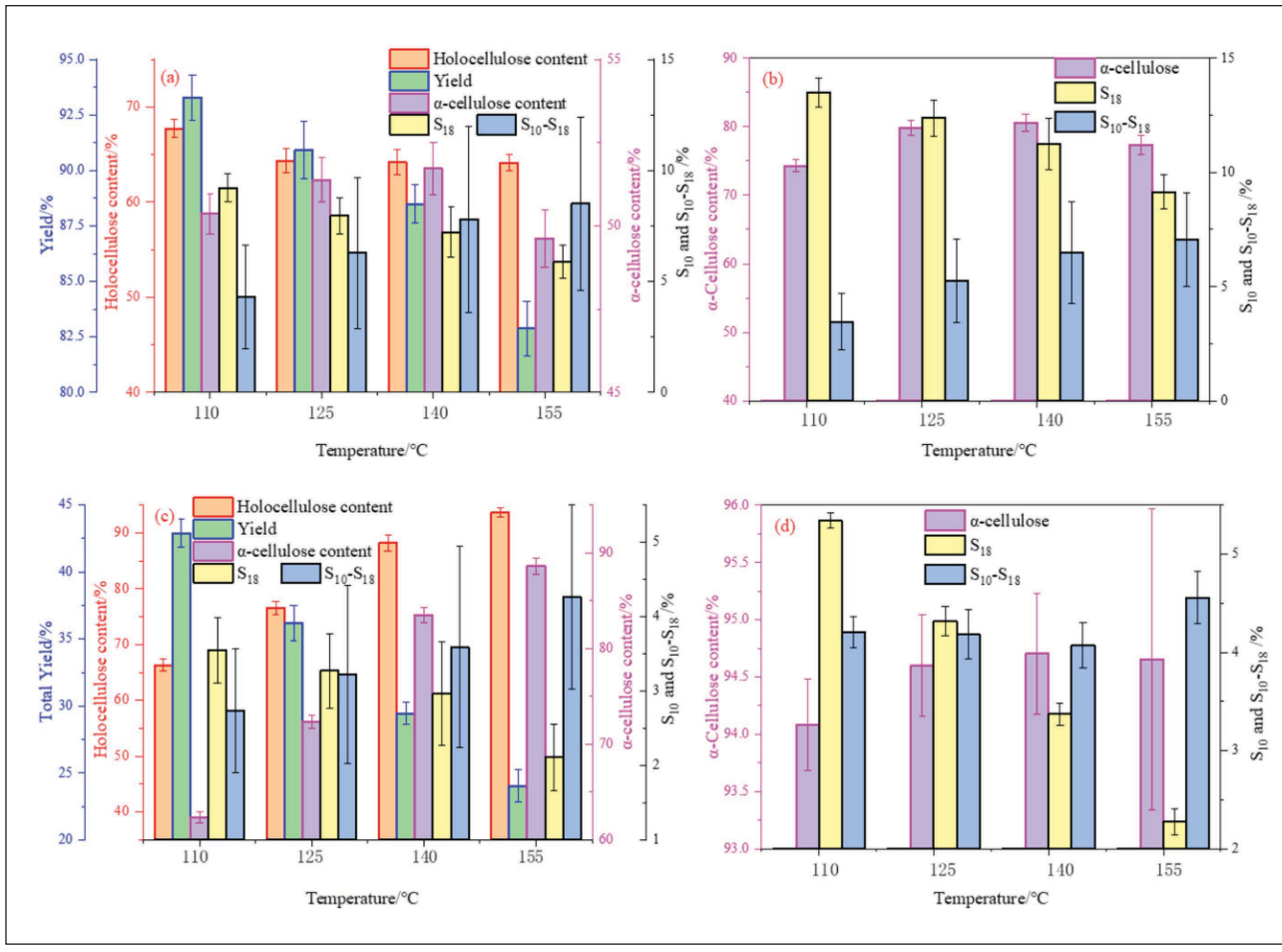

1. Influences of temperature on carbohydrate components of specimens after prehydrolysis and cooking: (a) based on specimen after prehydrolysis; (b) based on holocellulose after prehydrolysis; (c) based on specimen after cooking; and (d) based on holocellulose after cooking.

matic degradation of carbohydrates at high temperatures. On the other hand, the lignin content in specimens increased with increasing temperature, as shown in Table III. This is attributed to the different reactivity between carbohydrates and lignin. During the acidic PTA prehydrolysis process, lignin exhibits lower activity compared with carbohydrates, and it is more difficult to be degraded and dissolved [19]. The α-cellulose content also remained within a relatively stable range when the temperature was below 140°C, and it exhibited a certain decrease when the temperature increased to 155°C. From another perspective, the α-cellulose content based on holocellulose increased with increasing temperature until 140°C and decreased at 155°C, as can be seen from Fig. 1b. This also indicated the weakened selectivity on carbohydrates under high temperature during the prehydrolysis phase.

For alkali solubility, it is generally considered that S_{10} represents hemicelluloses and short-chain cellulose; S_{18} is typical hemicelluloses, also known as α-cellulose; and S_{10}-S_{18} represents α-cellulose, most of which are short-chain cellulose [20]. During the prehydrolysis phase, S_{18} exhibited significant decrease with increasing temperature, indicating the intensive hydrolysis effect on hemicelluloses, whereas S_{10}-S_{18} increased with the increasing temperature. These trends can be observed both in Fig. 1a (based on specimens) and Fig. 1b (based on holocellulose). This may be attributed to the intensive depolymerization effect on long chain cellulose under high temperature. It seems that excessively high temperature does not favor the retention of long chain cellulose during the prehydrolysis phase.

Figures 1c and 1d show the influences of prehydrolysis temperature on carbohydrate components of specimens after cooking. What needs to be explained here is that the specimens could not be reduced to fibrous mass when the cooking temperature was below 130°C, according to the results of preliminary experiments. Thus, the cooking temperature was selected as 140°C. It is notable that the specimens could not be reduced to fibrous mass when the prehydrolysis temperature was 110°C and even at 125°C, without the addition of PTA during the prehydrolysis phase, as indicated in Table IV. However, with the incorporation of PTA, the specimens could be dissociated to fibrous mass after cooking, even with the prehydrolysis temperature maintained at 125°C. This indicates that the

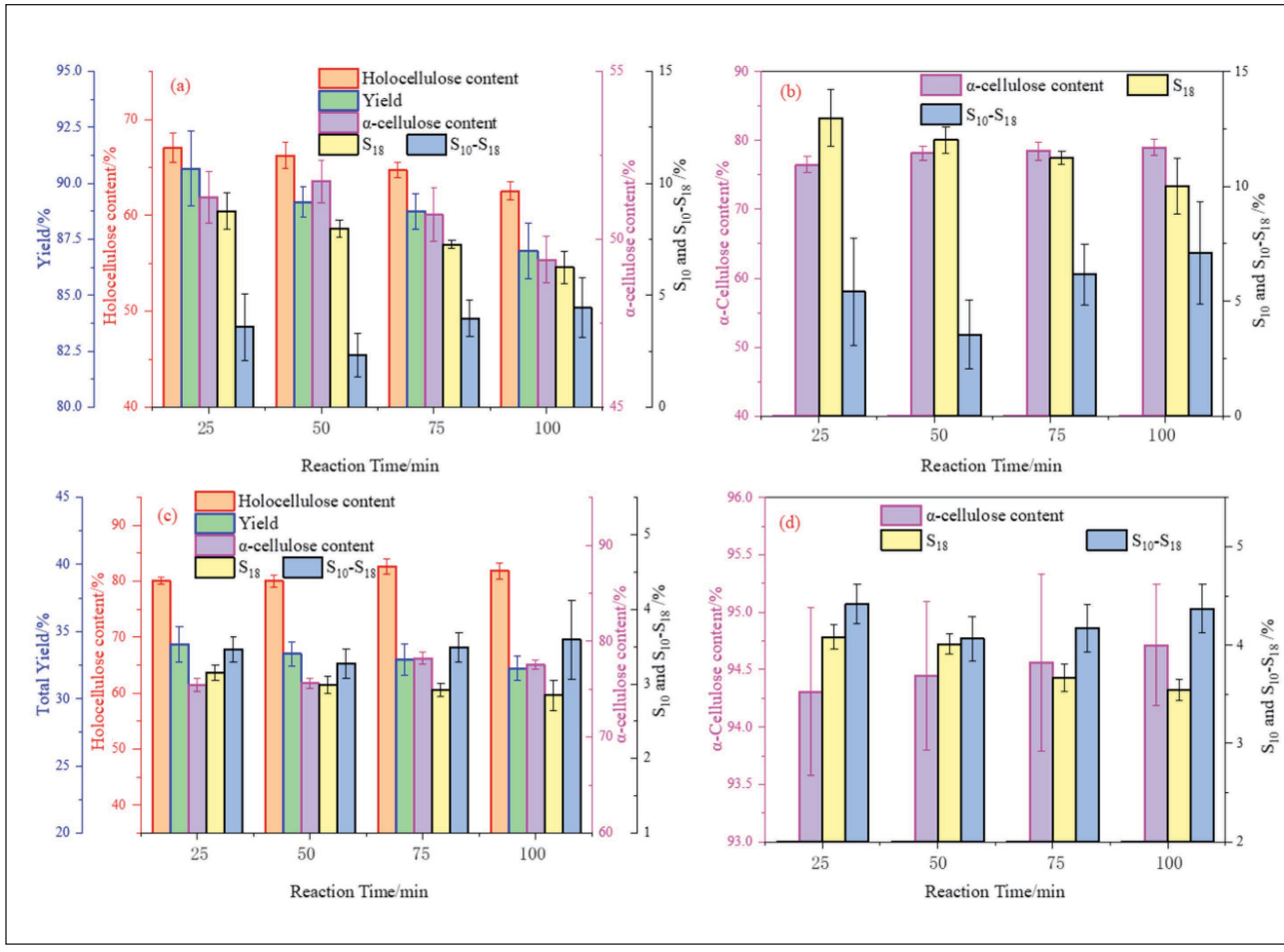

2. Influences of prehydrolysis reaction time on carbohydrate components of specimens after prehydrolysis and cooking processes: (a) based on specimen after prehydrolysis; (b) based on holocellulose after prehydrolysis; (c) based on specimen after cooking; and (d) based on holocellulose after cooking.

structure of lignin in raw materials was activated by the addition of PTA and is easily removed during the subsequent cooking process.

Due to the degradation of carbohydrates during the prehydrolysis phase, more lignin was exposed, and even deposited, on the surface of specimens. This resulted in a relatively high lignin removal ratio during cooking and increased holocellulose and α-cellulose contents based on specimens with increasing temperature, and it was also accompanied by a significant decrease of yield (Fig. 1c). Simultaneously, the α-cellulose content based on holocellulose also increased with increasing temperature and remained at a relatively high level (≥94.5%), as shown in Fig. 1d. This demonstrated that a specimen with relatively high cellulose purity can be obtained during cooking with PTA prehydrolysis treatment — one that achieves the qualitative requirements of dissolving pulp. However, the α-cellulose content based on holocellulose exhibited a slight decrease when the temperature increased from 140°C to 155°C. It can be inferred that long chain cellulose of specimens that were prehydrolyzed at a relatively high temperature suffered a stronger depolymerization effect during cooking. This is also demonstrated by the increased S_{10}-S_{18} component within the same temperature intervals. Furthermore, as indicated by Figs. 1c–1d, when the temperature gradually increased, S_{18} decreased rapidly, demonstrating the purification effect of the cooking process, which favors the qualitative enhancement of dissolving pulp.

Influences of reaction time

Figure 2 shows the influences of prehydrolysis reaction time on carbohydrate components of specimens after prehydrolysis and cooking. As indicated by Fig. 2a, both the yield and holocellulose content decreased with prolonged reaction time. It is notable that the α-cellulose content based on specimens showed a declining trend, while the α-cellulose content based on holocellulose exhibited a slight increase with prolonged reaction time, as indicated by Fig. 2b. Although α-cellulose suffered degradation to a certain extent during the prehydrolysis phase, the resistance of α-cellulose to hydrolysis is higher than that of hemicelluloses.

For alkali solubility, S_{18} decreased gradually with pro-

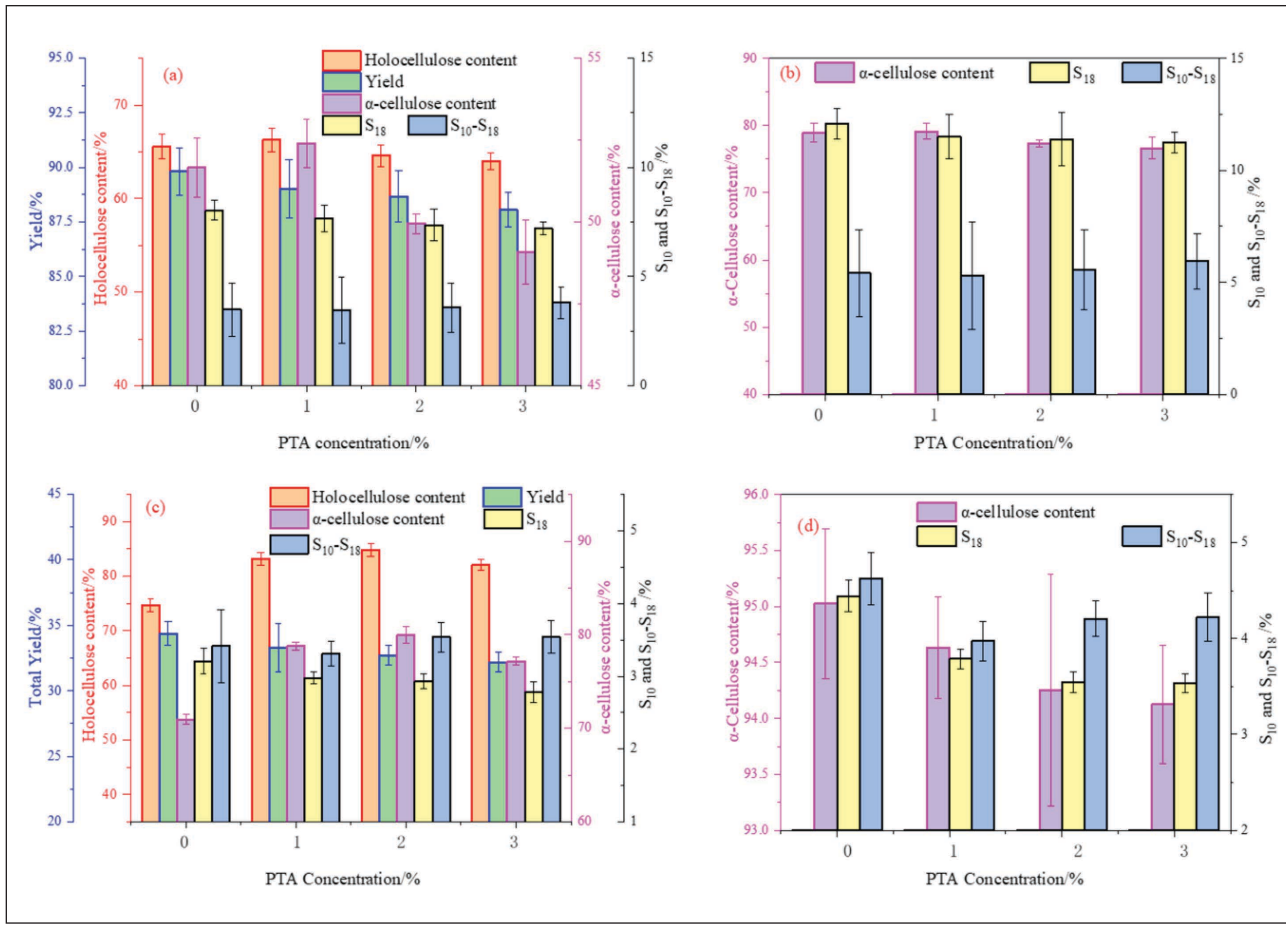

3. The influences of phosphotungstic acid (PTA) concentration on carbohydrate components of specimens after prehydrolysis and cooking: (a) based on specimen after prehydrolysis; (b) based on holocellulose after prehydrolysis; (c) based on specimen after cooking; and (d) based on holocellulose after cooking.

longed reaction time, demonstrating the serious degradation of hemicelluloses. Moreover, S_{10}-S_{18} displayed a tendency to decrease at the initial phase and increased later, with the minimum value appearing when the reaction time was 50 min. This indicated that the depolymerization of long chain cellulose was aggravated with the prolonged reaction time and also demonstrated that the reaction time should be controlled within a suitable range to retain the long chain cellulose.

The influences of reaction time on carbohydrate components of specimens after cooking are shown in Figs. 2c–2d. As can be seen from Fig. 2c, the holocellulose content, as well as the α-cellulose content, of the specimens increased with the initial increasing prehydrolysis reaction time, and the maximum values were achieved when the reaction time was 75 min. This was caused by the dissolution of lignin. With the prolonged reaction time during the prehydrolysis phase, more lignin was exposed on the surface of the specimens due to the degradation of hemicelluloses and was easily removed from specimens, thus resulting in increased holocellulose and α-cellulose contents based on specimens. Moreover, as mentioned previously, prolonged reaction time does not favor the retention of long chain cellulose during the prehydrolysis phase. Thus, with prolonged reaction time, the degradation rate of carbohydrates exceeded that of residual lignin, resulting in lower holocellulose and α-cellulose contents when the reaction time was 100 min.

In addition, as shown in Figs. 2c–2d, S_{18} and S_{10}-S_{18} both exhibited similar trends after cooking to those of prehydrolysis process. The drastic decline of S_{18} was attributed to the serious depolymerization of hemicelluloses, whereas the increased S_{10}-S_{18} when reaction time exceeded 50 min mainly originated from the depolymerization of long chain cellulose, which was further proof of the degradation of cellulose under prolonged prehydrolysis reaction time.

Influences of PTA concentration

Figure 3 shows the influences of PTA concentration on carbohydrate components of specimens after prehydrolysis and cooking. As shown in Fig. 3a, the yield and S_{18} of specimens decreased with increasing PTA concentration. This demonstrated that the carbohydrates, especially hemicelluloses, suffered an intensive hydrolysis effect with the in-

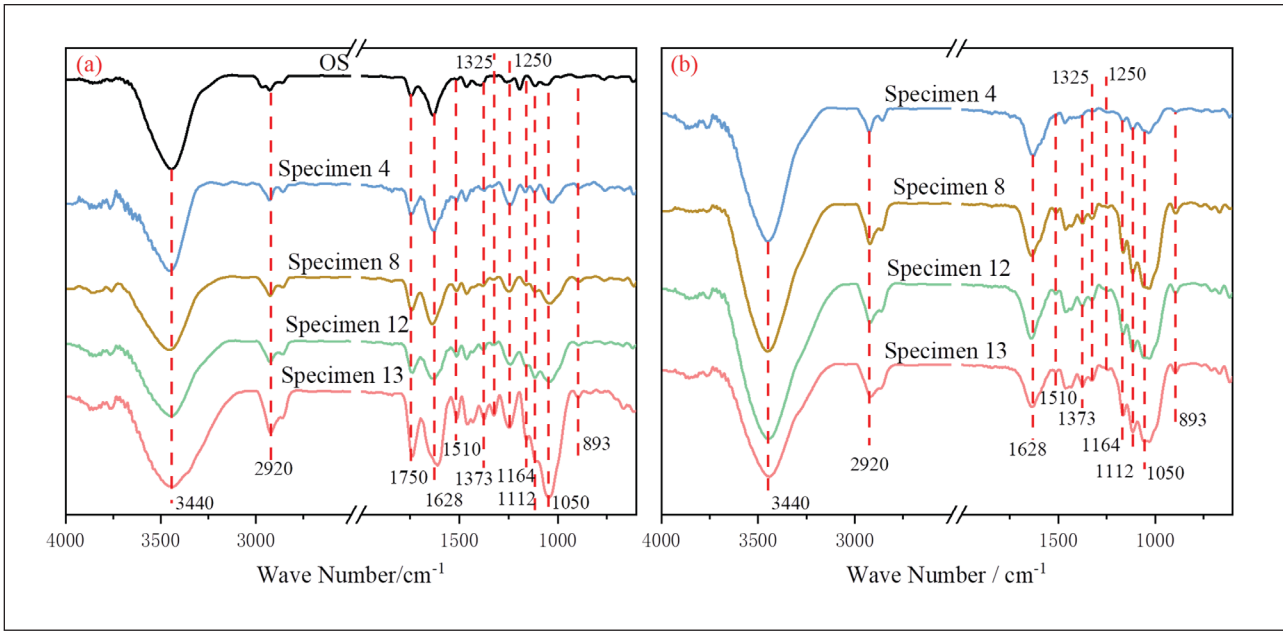

4. Fourier transform infrared (FTIR) spectra of specimens after (a) prehydrolysis and (b) cooking.

creasing system acidity. It is interesting to note that when PTA concentration was 1 wt%, both the holocellulose and α-cellulose contents increased in comparison with those of specimens only treated by hot water. This might be attributed to the partial degradation of lignin. When system acidity initially increased, partial lignin macromolecules, including acid soluble lignin and lignin fraction with low molecular weight, were dissolved. Similar results can be observed during the preparation process of lignin-rich microcrystalline cellulose by high temperature liquid water extraction catalyzed by transition metal ions [21]. Then, the holocellulose and α-cellulose contents decreased with further increased PTA concentration. During the PTA prehydrolysis phase, the residual lignin in specimens was relatively stable under acidic conditions, whereas the carbohydrates were further hydrolyzed by the catalytic effect of PTA, resulting in lower carbohydrate contents. In addition, the S_{10}-S_{18} remained within a relatively stable range but exhibited a slight increase depending on whether it was based on specimen or holocellulose, as indicated by Fig. 3a or Fig. 3b. This demonstrated that the concentration variation of PTA did not exhibit significant influence on the hydrolysis resistance of cellulose.

The influences of PTA concentration on carbohydrate components of specimens after cooking are shown in Figs. 3c–3d. In comparison with the specimens that were pretreated only by hot water, the holocellulose and α-cellulose contents of specimens both exhibited a significant increase with the incorporation of PTA, although the yield decreased. This indicated that the delignification selectivity was improved by the addition of PTA. However, both the holocellulose and α-cellulose contents of specimens decreased when PTA loading exceeded 2 wt%, demonstrating that excessive PTA loading during the prehydrolysis phase could not promote the lignin removal ratio but accelerated the carbohydrate degradation during the cooking process. A possible reason for this is that the crystalline region of cellulose was partially destroyed under relatively high acidity during the prehydrolysis phase [22], and it was easily depolymerized during the following cooking process.

For alkali solubility, S_{10}-S_{18} of specimens that were prehydrolyzed by 1 wt% PTA decreased to a certain degree compared with the specimens without the addition of PTA, whereas they increased with further increasing PTA concentration, as indicated by Fig. 3d. This also proved the previously mentioned inference, i.e., that the delignification selectivity could not be further improved by excessive PTA loading during the prehydrolysis process.

Structural characteristics

Figure 4 plots the FTIR spectra of specimens after prehydrolysis and cooking. As indicated by Fig. 4a, the absorption peaks of 1164 cm^{-1}, 1112 cm^{-1}, and 1050 cm^{-1} are caused by the stretching vibration of C–O–C, which are generally considered as typical absorption peaks of cellulose [23]. The absorption band at 893 cm^{-1} is typical of the β-linkage within glucose polymers between sugar units [24]. These peaks can be clearly observed in the spectra of specimens after prehydrolysis, indicating that more basic structural units of cellulose were exposed after prehydrolysis. The absorption bands at 2920 cm^{-1} and 1373 cm^{-1} are related to the stretching vibration bands of –CH in the $–CH_2$ and $–CH_3$ groups, respectively. These two bands also showed a remarkable increase after prehydrolysis. Furthermore, the absorption peak near 1628 cm^{-1} corresponds to the –CHO stretch vibration. The increased intensity of these absorp-

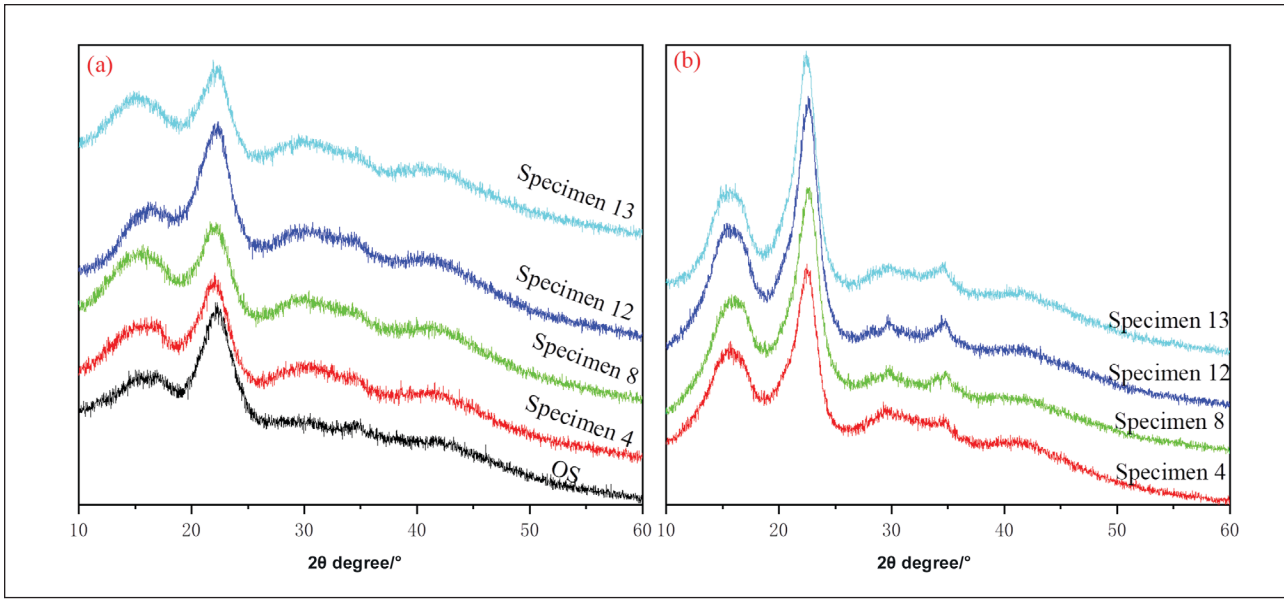

5. X-ray diffraction (XRD) spectra of specimens after (a) prehydrolysis and (b) cooking.

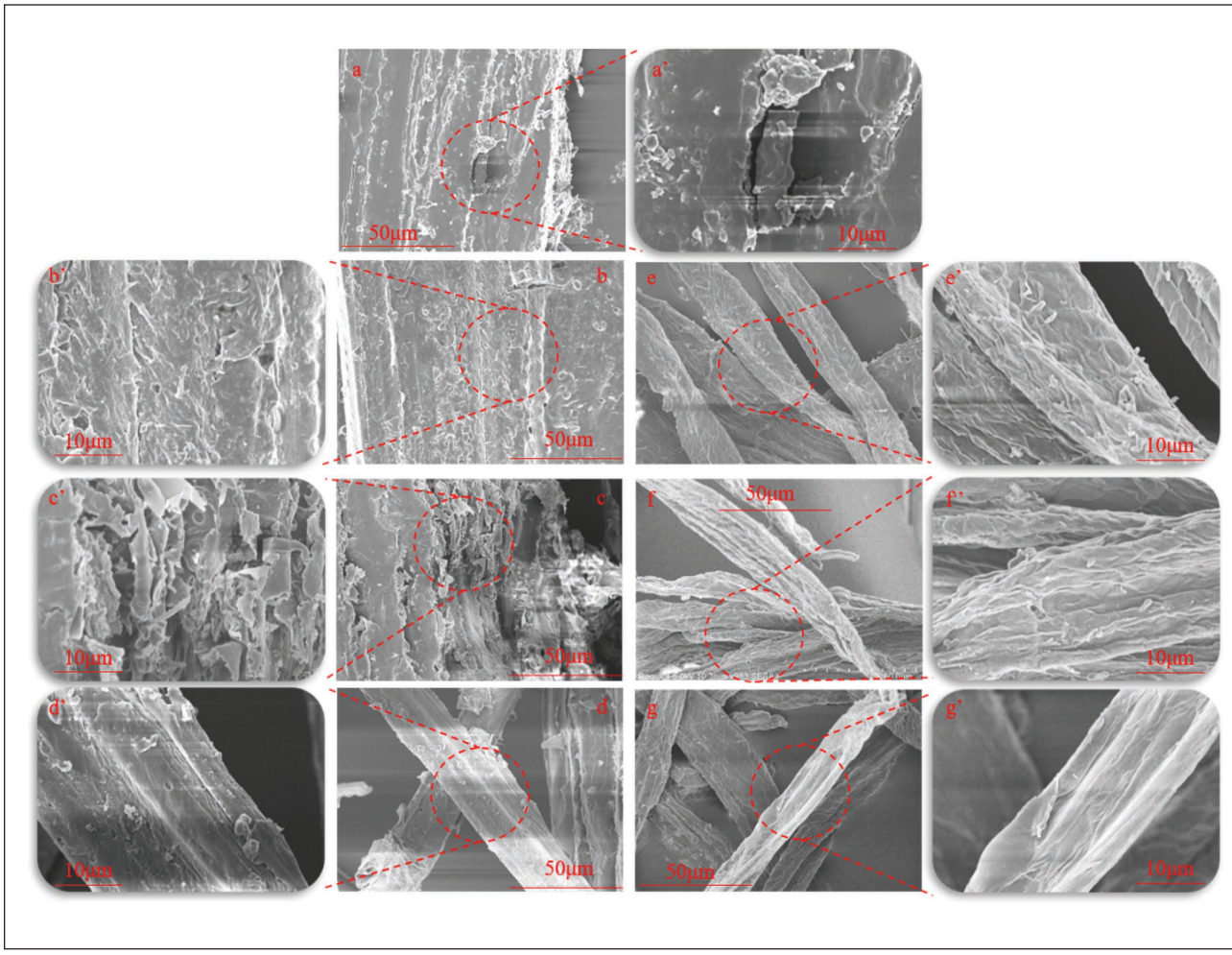

6. SEM images of (a) untreated grape branches (OS); and specimens after (b-d) prehydrolysis and (e-g) cooking under different magnification. Among them, (b) and (e) are specimen 8 after prehydrolysis and cooking, respectively; (c) and (f) are specimen 12 after prehydrolysis and cooking, respectively; (d) and (g) are specimen 13 after prehydrolysis and cooking, respectively.

tion peaks might be attributed to breakage of the cellulose backbone and the increase of –CHO groups during the prehydrolysis process. Although the relative content of lignin in specimens increased, the cellulose structure was loosened, and more reactive groups were exposed under the catalysis effect of PTA, resulting in the enhanced absorption peaks for cellulose after prehydrolysis.

In addition, the absorption peak of 1750 cm^{-1} is related to the –C=O groups unconjugated to aromatic rings. The peak at 1510 cm^{-1} corresponds to the aromatic C=C stretch of the aromatic rings of lignin [25]. Moreover, the absorption peaks at 1250 cm^{-1} and 1325 cm^{-1} represent the stretching vibration of guaiacyl (G) and syringyl (S) units, respectively. These absorption peaks are weakened and even disappeared after cooking, demonstrating that lignin was greatly removed during the cooking process.

Figure 5 shows the XRD patterns of OS and the specimens after prehydrolysis and cooking. It can be clearly seen that they exhibited similar diffraction patterns. There are three main diffraction peaks at 2θ=15.1°, 16.4°, and 22.6° for all specimens, which correspond to (1-10), (110), and (200) crystal planes, respectively [26,27]. Moreover, the diffraction peak at 22.6° in the XRD pattern of specimens after cooking became sharper, as shown in Fig. 5b, which indicates a higher crystallinity after cooking [28]. Also, the diffraction peak at 2θ=34.5° that represents (004) crystal plane appeared in the XRD patterns of specimens after cooking. Obviously, the crystalline structure of specimens after hydrolysis or cooking had not changed and remained cellulose I.

Morphological characterization

Figure 6 shows the SEM images of selected specimens after prehydrolysis and cooking. As can be seem from Fig. 6a, OS exhibited compact morphological structure with a relatively smooth surface, whereas the integral structure of specimens gradually changed to become looser after prehydrolysis. Moreover, the more intensive the prehydrolysis conditions, the more loose the structure that was observed. It is notable that the fiber cells of specimens treated at relatively high temperature (Fig. 6d) were separated after prehydrolysis, although the cells always maintained relatively high lignin content. In addition, as can be seen from Fig. 6d, spherical lignin exudates attached on the fiber surface could be observed in the magnified SEM image. It has been reported that thermochemical pretreatments reaching temperatures above the range for lignin phase transition caused lignin to coalesce into larger molten bodies that migrated within and out of the cell wall and redeposited on the surface of plant cell walls [29,30]. The spherical exudates on the fiber surface might be attributed to the redeposited lignin under high temperature. The hydrophobic lignin, which was melted and repolymerized during pretreatment, tends to form droplets to minimize its exposed surface in contact with aqueous solution.

As can be seen from Figs. 6e–6g, all the selected specimens were dissociated to fibrous mass after cooking. Moreover, with enhanced prehydrolysis conditions, a smoother surface and less deposited lignin particles can be observed in the SEM images of specimens, indicating the satisfactory pulp quality after the cooking process.

Prehydrolysis temperature optimization

Based on the results of the orthogonal experiment, temperature is the most important factor for PTA prehydrolysis. In order to obtain the optimal prehydrolysis temperature, a further optimized experiment focused on the prehydrolysis temperature using constant cooking and bleaching conditions was conducted.

Figure 7 illustrates the influence of prehydrolysis temperature on the carbohydrate components of specimens within the range of 130°C to 150°C during various treatment phases. As shown in Figs. 7a–7b, the maximum value for α-cellulose content of specimens, whether based on specimens or holocellulose, appeared when the prehydrolysis temperature was 145°C. During the cooking process, the α-cellulose content based on specimens also increased with the increasing temperature, whereas the α-cellulose content based on holocellulose achieved the maximum value when the prehydrolysis temperature was 145°C, as shown in Figs. 7c–7d. Moreover, the highest α-cellulose content of specimens after bleaching appeared at 145°C (94.04%), achieving the quality standards for dissolving pulp, and then decreased to a certain degree when the prehydrolysis temperature increased to 150°C (Fig. 7e). These findings are consistent with the results of the orthogonal experiment, indicating that excessive degradation of cellulose might be caused by the intensive prehydrolysis conditions.

During the cooking and bleaching phases, the total yield exhibited a significant decrease, typically decreasing from 29.0% to 26.1% when the prehydrolysis temperature increased from 145°C to 150°C. This is also consistent with the results of the orthogonal experiment and indicates the excessive degradation of cellulose, further resulting in decreased yield during the subsequent process. This can also be demonstrated by the increased S_{10}-S_{18} within the same temperature intervals. Furthermore, the DP of bleached specimens was measured, and the DP of specimens after bleaching was 853 when the prehydrolysis temperature was 145°C and exhibited a further decrease under 150°C. This is consistent with the results of carbohydrate components after prehydrolysis and cooking. It seems that 145°C can be selected as the optimum prehydrolysis temperature.

CONCLUSIONS

Dissolving pulp of a relatively high-quality grade can be prepared by grape branches via a PTA prehydrolysis kraft process. The lignin in grape branches can be efficiently activated by PTA prehydrolysis treatment, and relatively

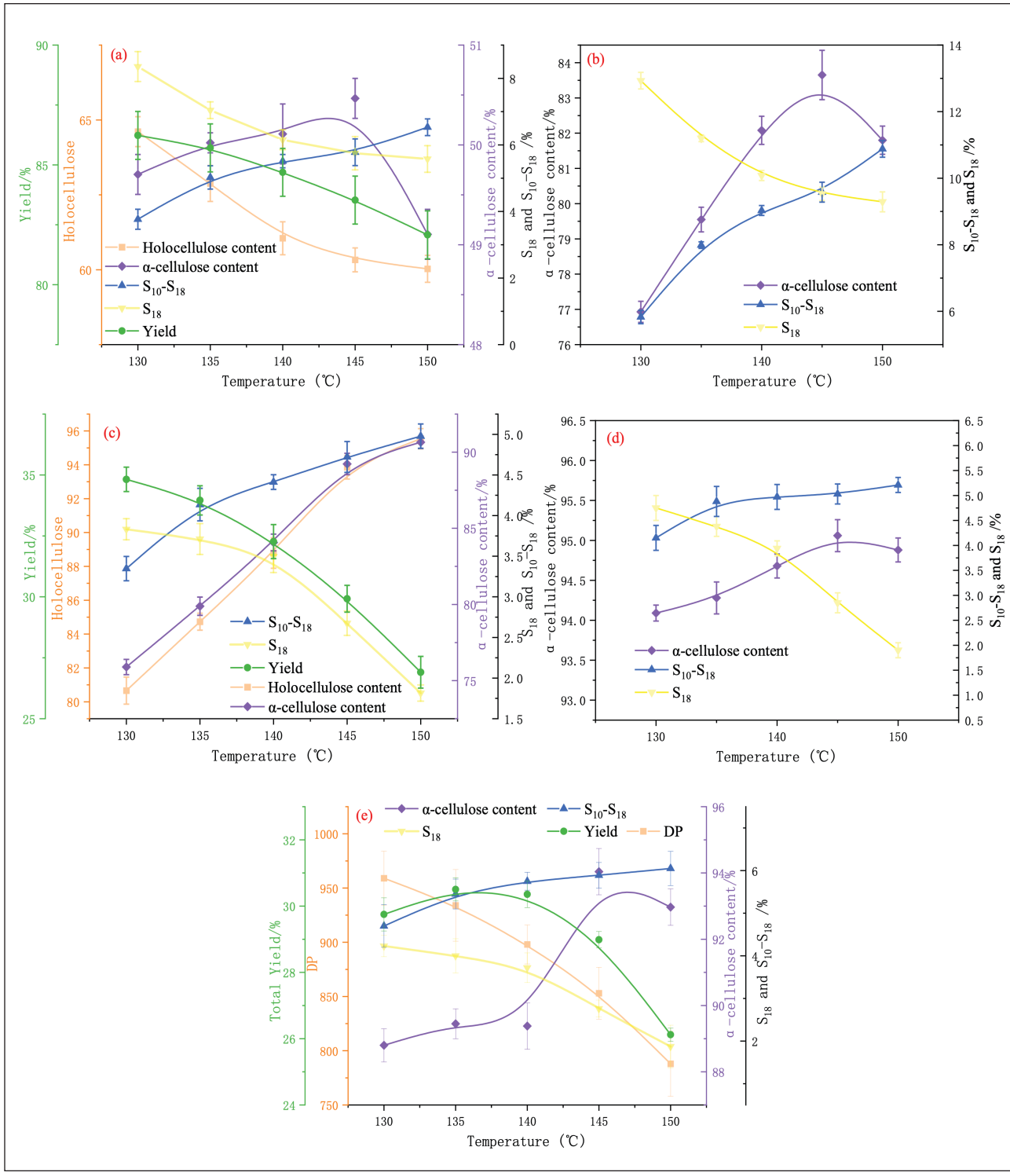

7. The influences of prehydrolysis temperature on carbohydrate components of specimens: (a) based on specimen after prehydrolysis; (b) based on holocellulose after prehydrolysis; (c) based on specimen after cooking; (d) based on holocellulose after cooking; and (e) based on specimen after bleaching.

mild conditions can be used during the subsequent cooking process.

Among the process variables during prehydrolysis, temperature exhibited the most significant influence on the cellulose purity of the obtained pulp fibers after cooking, followed by reaction time and PTA concentration. The elevation of prehydrolysis temperature favored the enhancement of pulp quality after cooking. However, serious degradation of long chain cellulose occurred under excessively high prehydrolysis temperature or prolonged

reaction time. In addition, the incorporation of PTA improved the delignification selectivity during the cooking process, whereas the delignification selectivity could not be further improved by excessive PTA loading.

The optimized prehydrolysis conditions were as follows: prehydrolysis temperature, 145°C; reaction time, 75 min; and PTA concentration, 1 wt%. Under these prehydrolysis conditions, 94.1% and 29.0% for α-cellulose content and total yield can be achieved after the given cooking and bleaching conditions, respectively. **TJ**

ACKNOWLEDGMENTS

The authors are grateful for financial support from the Natural Science Basic Research Program of Shaanxi Province (Grant No. 2020JQ-991).

LITERATURE CITED

1. Zhou, S., Li, Y., Huang, L., et al., *BioResources* 13(2): 2861(2018). https://doi.org/10.15376/biores.13.2.2861-2870.
2. Chen, Z.C., Zhang, H.W., He, Z.B., et al., *BioResources* 14(4): 7627(2019).
3. Nayeem, J., Jahan, M.S., Popy, R.S., et al., *TAPPI J.* 18(5): 287(2019). https://doi.org/10.32964/TJ18.5.287.
4. Borrega, M., Nieminen, K., Sixta, H., *BioResources* 6(2): 1890(2011).
5. Wang, G.S., Lee, J.-W., Zhu, J.Y., et al., *Appl. Biochem. Biotechnol.* 163(5): 658(2011). https://doi.org/10.1007/s12010-010-9071-4.
6. Galadima, A. and Muraza, O., *Int. J. Energy Res.* 39(6): 741(2015). https://doi.org/10.1002/er.3257.
7. Li, X., Lu, X., Nie, S., et al., *Ind. Crops Prod.* 145: 112154(2020). https://doi.org/10.1016/j.indcrop.2020.112154.
8. Qu, H., Liu, B., Li, L., et al., *Fuel Process. Technol.* 199: 106272(2020). https://doi.org/10.1016/j.fuproc.2019.106272.
9. Wang, X., Duan, C., Feng, X., et al., *Sep. Purif. Technol.* 266: 118562(2021). https://doi.org/10.1016/j.seppur.2021.118562.
10. Torlopov, M., Udoratina, E., Martakov, I., et al., *Cellulose* 24(5): 2153(2017). https://doi.org/10.1007/s10570-017-1256-3.
11. Chen, B.-H., Wang, Z.-Q., Jin, Z.-C., et al., *Biomass Convers. Biorefin.* (2021). https://doi.org/10.1007/s13399-021-01849-4.
12. Xiao, Z., Zhang, Q., Wang, X., et al., *Biomass Convers. Biorefin.* 10(4): 1007(2020). https://doi.org/10.1007/s13399-019-00518-x.
13. Zhang, J., Liu, X., Sun, M., et al., *ACS Catal.* 2(8): 1698(2012). https://doi.org/10.1021/cs300342k.
14. Demesa, A.G., Laari, A., Sillanpää, M., et al., *Molecules* 22(10): 1625(2017). https://doi.org/10.3390/molecules22101625.
15. Du, B., Liu, B., Yang, Y., et al., *Catalysts* 9(5): 399(2019). https://doi.org/10.3390/catal9050399.
16. Guo, Z., Li, D., You, T., et al., *ACS Sustainable Chem. Eng.* 8(32): 12110(2020). https://doi.org/10.1021/acssuschemeng.0c03491.
17. Du, B., Chen, C., Sun, Y., et al., *RSC Adv.* 10(52): 31479(2020). https://doi.org/10.1039/D0RA05069E.
18. Mateos-Espejel, E., Radiotis, T., Jemaa, N., *TAPPI J.* 12(3): 29(2013). https://doi.org/10.32964/TJ12.2.29.

ABOUT THIS PAPER

Cite this article as:
Li, T., Ma, Y., and Zhang, J.K., *TAPPI J.* 21(1): 35(2022). https://doi.org/10.32964/TJ21.1.35

DOI: https://doi.org/10.32964/TJ21.1.35

ISSN: 0734-1415

Publisher: TAPPI Press

Copyright: ©TAPPI Press 2021

About this journal

ABOUT THE AUTHORS

Equipment corrosion and acid recovery hinders further development of dilute acid prehydrolysis during the prehydrolysis kraft (PHK) cooking process. Considering its unique physicochemical properties such as high Brønsted acidity, high stability, and reusability, phosphotungstic acid (PTA) was expected to be used as a catalyst in the prehydrolysis phase of the PHK process for dissolving pulp preparation.

We found that lignin can be efficiently activated by PTA prehydrolysis treatment and is easily removed during the cooking process. Under optimized prehydrolysis conditions, relatively mild conditions can be used during the subsequent cooking process. Thus, PTA prehydrolysis represents an alternative approach for preparing a PHK dissolving pulp product. Our next step is to characterize and illustrate the structural variation of lignin during the PTA prehydrolysis process and to provide more information on this pretreatment approach.

Li

Ma

Zhang

Li is associate professor, Ma is lecturer, and Zhang is professor at the Institute of Chemical Engineering, Shaanxi Institute of Technology, Xi'an, Shaanxi, China. Email Li at l1tao@163.com.

19. Yue, X., He, J., Xu, Y., et al., *Carbohydr. Polym.* 208: 115(2019). https://doi.org/10.1016/j.carbpol.2018.12.072.

20. Miao, Q., Chen, L., Huang, L., et al., *Bioresour. Technol.* 154: 109(2014). https://doi.org/10.1016/j.biortech.2013.12.040.

21. Yue, X., He, J., Li, T., et al., *Cellulose* 28(3): 1405(2021). https://doi.org/10.1007/s10570-020-03620-w.

22. Wang, X., Duan, C., Zhao, C., et al., *Bioresour. Technol.* 253: 182(2018). https://doi.org/10.1016/j.biortech.2018.01.022.

23. Elanthikkal, S., Gopalakrishnapanicker, U., and Varghese, S., *Carbohydr. Polym.* 80(3): 852(2010). https://doi.org/10.1016/j.carbpol.2009.12.043.

24. Zhong, C., Wang, C., Wang, F., et al., *Carbohydr. Polym.* 136: 979(2016). https://doi.org/10.1016/j.carbpol.2015.10.001.

25. Agblevor, F.A., Ibrahim, M.M., and El-Zawawy, W.K., *Cellulose* 14(3): 247(2007). https://doi.org/10.1007/s10570-006-9103-y.

26. Ren, H., Shen, J., Pei, J., et al., *Cellulose* 26(15): 8367(2019). https://doi.org/10.1007/s10570-019-02712-6.

27. Trache, D., Khimeche, K., Mezroua, A., et al., *J. Therm. Anal. Calorim.* 124(3): 1485(2016). https://doi.org/10.1007/s10973-016-5293-1.

28. Lu, Q., Tang, L., Lin, F., et al., *Cellulose* 21(5): 3497(2014). https://doi.org/10.1007/s10570-014-0376-2.

29. Donohoe, B.S., Decker, S.R., Tucker, M.P., et al., *Biotechnol. Bioeng.* 101(5): 913(2008). https://doi.org/10.1002/bit.21959.

30. Ko, J.K., Kim, Y., Ximenes, E., et al., *Biotechnol. Bioeng.* 112(2): 252(2014). https://doi.org/10.1002/bit.25349.